CONF-800804--2

AN EVALUATION OF CLAMP EFFECTS ON LMFBR PIPING SYSTEMS

Gerald L. Jones

Swanson Engineering Associates Corporation

McMurray, Pennsylvania

ABSTRACT

Loop-type liquid metal breeder reactor plants utilize thin-wall piping to mitigate through-wall thermal gradients due to rapid thermal transients. These piping loops require a support system to carry the combined weight of the pipe, coolant and insulation and to provide attachments for seismic restraints. The support system examined here utilizes an insulated pipe clamp designed to minimize the stresses induced in the piping. To determine the effect of these clamps on the pipe wall a non-linear, two-dimensional, finite element model of the clamp, insulation and pipe wall was used to determine the clamp/pipe interface load distributions which were then applied to a three-dimensional, finite element model of the pipe. The two-dimensional interaction model was also utilized to estimate the combined clamp/pipe stiffness.

INTRODUCTION

To minimize the potential for local discontinuity stresses and buckling in the thin-walled liquid metal piping, a non-integral insulated pipe clamp was designed to serve as attachment points for load hangers and seismic restraints. These clamps are composed of two semi-circular bands with bolt flanges, gussets and attachment lugs welded to the bands, as shown in Figure 1. In addition to these metal outer bands, there are two semi-circular bands of sheathed load-bearing insulation attached to the inner surface of the clamp, which thermally isolates the metal clamp from the pipe. This assembly is held in place by bolts and Belleville spring stack-ups that are preloaded at assembly to produce an initial contact pressure between the clamp assembly and the surface of the pipe. The Belleville spring stack-ups are designed to accommodate the thermal expansion of the pipe without inducing large changes in the bolt/spring loads or the contact pressure at the pipe/clamp interface. This is accomplished by designing the spring stack-up so that the load-deflection curve has a relatively flat response region in the vicinity of the selected preload. The original design considerations for the Clinch River Breeder Reactor Plant (CRBRP) In-Containment piping and clamps are described in detail in Reference (1)*. The primary and in-containment intermediate heat transport pipe loop geometry for CRBRP is also shown in this paper. Although there are five unique clamp sizes used on this piping, this paper will only cover the 24" x 6" (610 mm x 150 mm) clamp. The basic procedure used to analyze the other clamp sizes is the same as that discussed here. A detailed description of the CRBRP pipe clamps is given in Reference (2) and a typical support arrangement for the CRBRP in-containment piping is shown in Figure 2. Other combinations of constant load hangers and snubbers are used also. The load ratings for each clamp size is given in Table 1 but it should be pointed out that these load ratings are dependent upon the pipe geometry for thin walled piping.

* Numbers in parentheses designate References at the end of the paper.

TABLE 1
MAXIMUM LOAD RATINGS FOR CRBRP IN-CONTAINMENT PIPE CLAMPS

Clamp Size Diameter x Width	Preload (lbs)	Normal & Upset Loads (lbs) (1)	Emergency Loads (lbs) (1)	Faulted Loads (lbs) (1)
24 x 6	20,000	11,100	13,300	20,000
24 x 8	26,600	14,800	17,700	26,600
24 x 12	40,000	22,200	26,600	40,000
36 x 8	28,800	16,000	19,200	28,800
36 x 12	43,200	24,000	28,800	43,200

1 in. = 25.4 mm 1 lb. = 4.448 N

NOTES: (1) The loads listed are the maximums for a single load applied either parallel to the clamp split line or perpendicular to the clamp split line. For thin walled piping these load ratings are dependant on the pipe geometry.

For combined loadings the magnitude of the resultant load vector should not exceed the values listed above.

Even though these clamps were designed to minimize any effects on the CRBRP piping, the stresses induced in the pipe wall by the clamp loads are still significant and must be evaluated. Therefore, it was necessary to determine the interaction loads between the clamp and the pipe and the induced local pipe stresses. The purpose of this paper is to describe the procedure utilized to determine the effect of the clamps on the CRBRP piping.

ANALYTICAL PROCEDURE

Since the clamp assembly (clamp band and insulation band) is slightly larger in diameter than the outside diameter of the pipe (nominally 0.075 inches (1.905 mm) greater) and because the pipe wall and the portion of the clamp band between the load lugs and the bolt flange gussets are relatively flexible, the distribution of contact pressure acting on the clamp/pipe interface is complex and is a non-linear function of preload, differential thermal expansion, and externally-applied loads. Therefore, a non-linear, finite element model was set up to determine the pipe-to-clamp interface load distribution due to preloads, external loads and thermal expansion. These interface load distributions were then applied to a three-dimensional shell model of the pipe to determine the local pipe wall stress state. A general purpose finite element code named WECAN (3) was used for both these models. This procedure and the models described are similar to those previously described in Reference (4).

CLAMP/PIPE INTERACTION MODEL

The 2-D interaction model used to determine the circumferential interface load distribution between the pipe and the clamp is shown in Figure 3. The pipe is represented by 74 beam elements which cover a span of 5^{o} each, with the exception of the elements adjacent to the clamp split line which cover a span of 3.2^{o} under the split line and 3.4^{o} on each side of the split

line. Since this is a 2-D dimensional model, the bending stiffness of these beam elements must be modified to reflect the difference in stiffnesses between the equivalent ring composed of beam elements and the actual stiffness of the pipe.

Matching the stiffness of the equivalent ring with that of the pipe was accomplished by iterative process in which an attempt was made to match the radial deflections between the equivalent 2-D finite element ring model of the pipe with different effective lengths and a 3-D finite element shell model of the pipe for a simple load case. The 3-D shell model of the pipe is shown in Figure 4. This particular model is 144 inches (3.66 m) long which was considered to be sufficiently long enough that the effect of the end conditions could be neglected.

The clamp band is also modeled with beam elements having the same arc lengths as the corresponding pipe elements. For these elements, the actual cross-section properties of the clamp band are used. The attachment pads, bolt flanges and flange gussets are modeled with shell elements. For these elements the actual cross-section properties were also used. However, the thickness used for the attachment pads and the bolt flange gussets were doubled to account for the presence of two flanges and two load ears at each location.

The clamp band and the pipe beam elements are connected by several dynamic spring-gap elements. The spring represents the equivalent insulation stiffness, and the gaps are given a distribution which corresponds to the worst case mismatch between the maximum/minimum radii of the pipe O.D., the insulation band I.D./O.D. and the clamp band I.D. To simplify the analysis, the gap distribution between the insulation band O.D. and the clamp band I.D. is simply added to the gap distribution due to the difference in radii between the pipe O.D. and the insulation band I.D.

The Belleville spring stackups were modeled with three dynamic spring gap elements in series, as shown schematically in Figure 5. The dynamic element was used because it allows a negative spring constant to be input, so that a decrease in the total spring constant can be modeled. The preload is induced in the interaction model by shifting the zero load point of the load-deflection curve in the negative direction by the amount required to produce the desired preload at a zero deflection. This is accomplished by inputting negative gaps for the spring-gap elements in the Belleville spring model.

The stop bolt stiffness used was based on an axial loading acting on a cross-sectional area defined by the root diameter of the threads. Since this bolt is installed after the clamp is preloaded, the initial gap for analysis was set equal to the differential deflection between the upper two bolt flanges for the preload only case. This means that the stop bolt gap should be zero under the preload only conditions but may open or close under thermal expansion or externally applied loads.

This 2-D interaction model does not account for the 3-dimensional effects of the clamp of the pipe. These 3-D effects are caused by the fact that there are two separated load ears and bolt flange gussets rather than one solid

piece as modeled. Also, the deflections of the pipe wall under the clamp band would be a function of the axial location with respect to the center of the clamp band. However, a finite element model, which would determine both the axial and circumferential interface load distributions, would be large and unwieldy. The axial effect discussed above is not considered to be significant, especially since all of the analysis completed has shown that the hoop stress is the critical stress component in every load case analyzed. Also, some preliminary work with the shell model of the pipe indicated that the maximum hoop stresses in the pipe wall were not very sensitive to the form of the axial distribution of the interface loads.

QUALIFICATION OF INTERACTION MODEL

In addition to the parametric studies comparing the deflections between an equivalent ring model and a 3-D shell model for a simple load case, an effort was made to qualify the 2-D finite element interaction model. This was accomplished by analyzing the preliminary thermal test of Reference (2) using the 2-D interaction model and comparing the differential radial deflections measured in the test with those predicted by the model. Since the preliminary clamp band had the same basic geometry as the prototype clamp, the clamp geometry was not changed. However, the preliminary thermal clamp test was performed with a piece of 24-inch (610 mm) O.D. pipe with a wall thickness of approximately 0.4 inches (10.2 mm) rather than the currently specified wall thickness of 0.5 inches (12.7 mm). Therefore, the thickness and bending moment of inertia of the pipe beam elements were modified to reflect the reduced pipe wall thickness used for the preliminary thermal clamp test.

A polar plot of the experimentally derived radial deflections and the analytically predicted radial deflections is shown in Figure 6. It can be seen that the two deformed shapes are virtually identical. Therefore, it was judged that modifying the bending stiffness for pipe beam elements based on an equivalent length of pipe was an appropriate method.

In an attempt to further verify this conclusion, the cold preload case for the 24" x 6" (600 mm x 150 mm) clamp was run with the interaction model. Then the resultant interface loads were applied to the 3-D shell model of the pipe as line loads at the outer edges of the clamp band. Radial deflections were extracted from both the interaction model and at the symmetry plane of the shell model. A comparison of these deflections is shown in Figure 7. This plot shows good agreement between the two models.

INTERACTION MODEL RESULTS

A large number of load combinations were investigated with the interaction model for one clamp size. The interface load distributions for these load cases were plotted and compared to determine which load cases were limiting. Two criteria were used to made this comparison; maximum load at any point around the pipe wall circumference and non-uniformity of the load distribution. The latter criterion was found to be important during early parametric studies conducted with the three-dimensional shell model of the pipe. It was found that the more uniform load distributions produced lower localized hoop bending stresses in the pipe wall. Since the hoop bending was found to be the critical stress component in every case, the uniformity of the

load distribution is as important a criteria as the peak interface load. However, because the matter of relative uniformity of the interface load can only be judged subjectively, the shell model was used to determine the critical load case where there was some question.

The interface load distributions and resultant deflections of the clamp and pipe cross-section are illustrated schematically in Figure 8 for increasing preloads. Note that most of the clamp deformation occurs in the region between the bolt flange gusset and the attachment lugs, whereas the pipe cross-section initially becomes slightly elliptical due to equal and opposite loads under the load lugs. Eventually, contact occurs under the bolt flanges at the top and bottom of the major elliptical axis as the preload is increased, then the deformed shape becomes an oblate ellipse. The effect of externally applied loads is to produce a shift of the basic preload pattern shown in the direction opposite from the resultant applied load. If the differential thermal expansion between the clamp and the pipe is included, then the interface loads become slightly more uniform around the circumference of the pipe. As the above discussion indicates, the clamp/pipe interaction is a highly non-linear problem, because both the peak interface pressures and the circumferential location of the peak pressures are a function of the applied load combinations. Typical 24" x 6" (610 mm x 150 mm) clamp interface load distribution plots are shown in Figures 9 through 14 for cold boltup preload plus thermal expansion and deadweight, and four faulted seismic load cases.

The interaction model was also utilized to calculate a combined clamp/pipe stiffness from the bolt flange deflections and attachment pad deflections for the external load cases. The clamp/pipe stiffnesses were calculated by dividing the applied load in each case by the appropriate deflection. The stiffness values obtained for the 24"x6" (610mm x 150mm) clamp are shown in Table 2 below. As shown in Table 2 the effective clamp/pipe stiffness is greatly reduced for loads applied along the split line of the clamp. In fact, the tensile split line load case stiffness is an order of magnitude lower than the other values. This occurs because the clamp separates from the pipe over a substantial area for this load case.

Table 2

Clamp/Pipe Stiffness for 24"x6" (610mm x 150mm) Clamp

Type of Load	Load Direction	Stiffness (lbs./in.)
Split Line Load	Tensile	2.5×10^4
	Compressive	2.7×10^5
Attachment Pad Load	Tensile	4.7×10^5
	Compressive	6.8×10^5

1 lbs./in. = 1.75×10^2 N/m

These stiffnesses were required for the seismic analysis of the CRBRP primary and intermediate heat transport system piping loops. The pipe/clamp stiffness is combined in series with the snubber stiffness and the structural steel stiffness to obtain an equivalent support stiffness used for the seismic models of the piping loops. Although it is common practice to use only one

support stiffness value for each seismic restraint, the clamp/pipe stiffness is a function of both the load direction (tension vs. compression in the support train) and the point of attachment to the clamp (loads acting along the clamp split line vs. loads acting on the attachment pads). Therefore, a refined seismic model might require the use of biaxial support stiffnesses which are a function of the associated support load train, load direction and angle of load application. This effect becomes more complex when two or more snubbers are attached to a given clamp. For this case, the resultant applied load on the clamp and the effective support stiffness becomes a function of time also since one support configuration could be in tension and the other in compression at some point during a seismic event or any combination of the two. There are an infinite number of load combinations which could occur in a seismic event. Accounting for this effect properly would require the use of a support stiffness matrix with the appropriate off diagonal coupling terms. In addition, separate tensile and compressive stiffnesses would have to be used. To analyze a piping loop with these complexities a non-linear, time-history piping model would be required for seismic analysis. This would add a large amount of complexity and expense to the seismic analysis of the piping loops. These effects are currently being handled in the seismic piping analysis by using minimum nominal support stiffness values with a linear seismic analysis model. This approach is based on previous parametric studies in which the critical seismic elbow stresses as a function of effective support stiffness were determined as reported in Reference (5). Further sensitivity studies to evaluate the effect of clamp stiffness variation on the pipe stresses are needed to verify the adequacy of using nominal stiffness values.

The interaction model was also used to check the stresses in the portion of the clamp band between the bolt flange gussets and the attachment pads, the clamp bolt loads and the peak interface pressures acting on the load- bearing insulation.

PIPE SHELL MODEL

The interface loads obtained from the 2-D interaction model are applied to a 3-D shell element model of the pipe such as that shown in Figure 15. The half shell model shown in Figure 15 is used for all load cases which produce symmetric interface load distributions such as preload, deadweight, thermal expansion, vertical seismic loads only, and horizontal seismic loads only. However, if both horizontal and vertical seismic loads are applied simultaneously, then the interface load distribution is no longer symmetric, and a full 360-degree shell model such as that shown in Figure 4 must be used.

The interface loads given by the interaction model are actually concentrated nodal loads equal to the integrated pressure loading over the width of the clamp and the average arc length on each side of each spring-gap element. To apply these loads to the shell model properly, the interface loads must be spread out over the load area in some manner. To do this the interface loads are applied to the shell model as nodal loads spread uniformly over the width of the clamp band. A FORTRAN preprocessor was written which generated a nodal load file for the shell model using the gap element forces from the interaction model.

The stresses obtained by this procedure are due to the clamp effects only. Therefore, these stress components must be combined with the global pipe stress state due to other effects such as deadweight, thermal expansion, internal pressure, through the wall thermal gradients and seismic loads to obtain the total stress state in the pipe. Before this can be done the clamp-induced stress components must be divided into appropriate categories (primary membrane, primary bending and secondary). Then the local clamp-induced stress components are combined with the global pipe stresses in a manner consistent with the ASME Code (6, 7), as modified by RDT Standard F9-4T (8). A FORTRAN post-processor is currently being developed to handle this combination procedure.

CLASSIFICATION OF PIPE STRESSES

For screening purposes the stresses induced in the pipe by loads such as preload, deadweight, and seismic loads are considered to be largely primary, and the stresses due to thermal expansion are secondary. However, since the clamp restricts the pipe deformation greatly, any localized yielding of the pipe wall would be partially alleviated by the ability of the clamp to redistribute the interface loads around the circumference of the pipe. This implies that some portion of the clamp-induced stress state is secondary in nature. Since the exact amount of secondary stress could not be determined and because it is not conservative to consider all of the clamp-induced stress as secondary, the following procedure was used to separate the pipe stresses into primary components and secondary components:

a. All of the membrane stress components are considered to be primary.

b. Due to the nature of the clamp/pipe interaction, only a portion of the bending stress component is considered to be primary. Although all of the bending components could be considered as secondary, this would not be conservative either. Therefore, a split similar to that used for elbows in NB-3685.4 of the ASME Code (6) was used. Namely, 75% of the bending stress components were classified as primary and 25% as secondary.

c. Thermal expansion effects were included in the normal operating and seismic load cases. No attempt was made to separate that portion of the stress state due to thermal expansion from the total stress other than the split discussed in (b) above.

d. Stress components due to pressure loading and thermal transients are not included in this analysis, because the overall piping analysis will include these effects as well as the global forces and moment due to applied loads.

The appropriate stress limits were taken from ASME Code Case 1592 (7) as modified by RDT F9-4T (8). It should be noted that the time independent stress limits were used for the seismic load cases. This is appropriate because seismic loads occur for short time periods, therefore, creep effects are not significant.

SHELL MODEL RESULTS

The stress contours at the outer surface of a 24 inch (610 mm) pipe with a 0.5 inch (12.7 mm) wall thickness due to cold boltup for a 6-inch (150 mm) wide by 0.5 inch (12.7 mm) thick clamp band are shown in Figures 16 and 17. The stresses at the inner surface are lower but have the same general pattern. Examination of Figures 16 and 17 shows that the hoop stress component is significantly higher than the axial component, and both components have alternating tensile and compressive regions around the circumference. This variation is a reflection of the interface load distribution. In general tensile stresses occur in regions where the pipe and clamp are not in contact, and compressive stresses occur in areas where contact does occur. Further examination shows that the maximum hoop stress is approximately 27.8 ksi (19.2Mpa), which is relatively high especially in light of the fact that the global pipe stresses are not accounted for. When the external load cases were run for the desired maximum clamp load rating, it was found that the combined pipe stresses for some cases would not meet the appropriate ASME Code limits. This was particularly true for the cases in which the load was applied to the bolt flanges with the load directed along the split line of the clamp.

Examination of the interaction model results indicated that the high pipe stresses were due to relatively high, narrow peaks in the interface pressure especially for the compressive, split line load case. It was determined that this occurs because the clamp band is too flexible. For compressive, split line loads this means that the bolt flanges dig into the pipe at the top of the clamp, whereas, tensile, split line loads cause the clamp band to pull away from the pipe. These flexibility effects would prevent the use of this clamp at the desired maximum load rating for certain load combinations.

STIFFER CLAMP DESIGN

To demonstrate that a stiffer clamp band would resolve the pipe stress problem, the critical seismic load cases were rerun with the bending stiffness of clamp band elements increased. Using a clamp band bending stiffness equivalent to that for a 1.5 inch (38 mm) thick band, the interface loads were distributed in a more uniform manner and the subsequent shell model runs showed substantially lower stresses. Since the maximum stress components were reduced considerably for this design, it was concluded that the combined pipe stresses will probably meet the appropriate ASME Code limits.

Using the stiffer clamp design provides a solution to the stress problems for the case of a seismic load acting along the split line of the clamp. A preferred clamp design concept, which increases the clamp band stiffness by using continuous gussets around the band is shown in Figure 18. Basically, continuous gussets, which run completely around the clamp band, were added. These gussets were designed to produce a moment of inertia at the minimum cross-section which is equivalent to the moment of inertia of a 1.5 inch (38 mm) thick band. Therefore, this design should be at least as stiff as the design with the thicker band. The analysis of this design configuration is currently underway using the same procedure described for the more flexible clamp. Preliminary results indicated that the clamp/pipe stiffnesses increased significantly for the revised design and that the directional

dependance and the coupling effect were also reduced. If fact some preliminary work indicates that the coupling effect is probably insignificant for a typical CRBRP support train, because the flexibility of the snubber becomes more dominant.

CONCLUSIONS

The problem of interaction between the sodium piping and the pipe clamps, which act as an interface between the CRBRP piping and the pipe support system, was solved by the use of two finite element models. One model used was a 2-D interaction model with gap elements from which the interface loads, bolt loads and clamp band stresses were obtained. The second model was a 3-D shell model of the pipe used to determine the local pipe wall stresses due to the clamp effect. This analysis indicated that 24-inch (610mm) clamps with more flexible bands produced overstress conditions in the pipe for some applications at the desired maximum load ratings. The combined clamp/pipe stiffnesses were also lower than desired for these load cases. Some additional analysis work using the same analytical methods on the stiffer clamp design indicates that the desired load ratings can be achieved for all planned applications. Additional advantages for the revised clamp design were increased piping system frequencies due to increased effective support stiffnesses and less pronounced directional stiffness and coupling effects.

ACKNOWLEDGEMENTS

This paper is based on work performed under subcontract to Westinghouse Electric Corporation, Advanced Reactors Division on U.S. Department of Energy Contract EY-76-15-2395. The author wishes to express his appreciation of the technical contributions made by R. M. Mello, L. P. Pollono and R. H. Mallett. A special word of thanks is given to Janice Hockenbery for typing the manuscript.

REFERENCES

1. L. P. Pollono and R. M. Mello, "Design Considerations for CRBRP Heat Transport System Piping Operating at Elevated Temperatures", ASME Paper 79-NE-5.

2. L. P. Pollono and R. M. Mello, "Design and Testing of CRBRP Insulated Horizontal and Vertical Pipe Clamps" to be presented at the ASME Century II, Emerging Technology Conference, San Francisco, California, August, 1980.

3. A. W. Filstrup, F. J. Bogden, S. K. Chan et. al., "WECAN-Westinghouse Electric Computer Analysis, User's Manual", Westinghouse R&D Report 78-1E7-NESPD-R1 February, 1978. (Availability: Westinghouse R&D Center, Pittsburgh, Pa.)

4. L. L. Hyde and S. E. Wagner, "The Effects of Support Clamps on Elevated Temperature Piping", 4th International Conference on Structural Mechanics in Reactor Technology, Vol. F, Paper F1/7, Commission of the European Communities, Brussels, 1977.

5. R. M. Mello and L. P. Pollono, "Evaluation of the Influence of Seismic Restraint Characteristics on Breeder Reactor Piping Systems", "Piping Restraint Effects on Piping Integrity", American Society of Mechanical Engineers, New York, 1979.

6. ASME Boiler and Pressure Vessel Code, ANSI/ASME BPV-III-NCA, Section III, Division 1, "Rules for Construction of Nuclear Power Plant Components", 1974 edition with addenda through Summer 1975. The American Society of Mechanical Engineers, New York, 1974.

7. "Class 1 Components in Elevated Temperature Service, Section III", Code Case 1592-7, ASME Boiler and Pressure Vessel, dated December 22, 1975.

8. RDT Standard F9-4T, "Requirements for Construction of Class 1 Elevated Temperature Nuclear System Components (Supplement to ASME Code Cases 1592, 1593, 1594, 1595 and 1596)", Amendment 4, April, 1977. (Availability: Oak Ridge National Laboratory, Reactor Standards Office.)

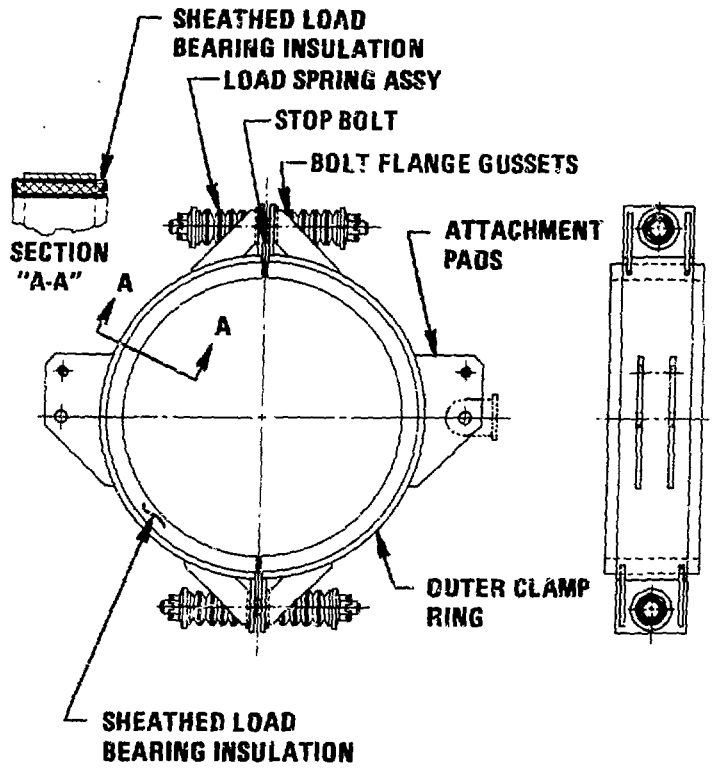

Figure 1 Horizontal Pipe Clamp Details

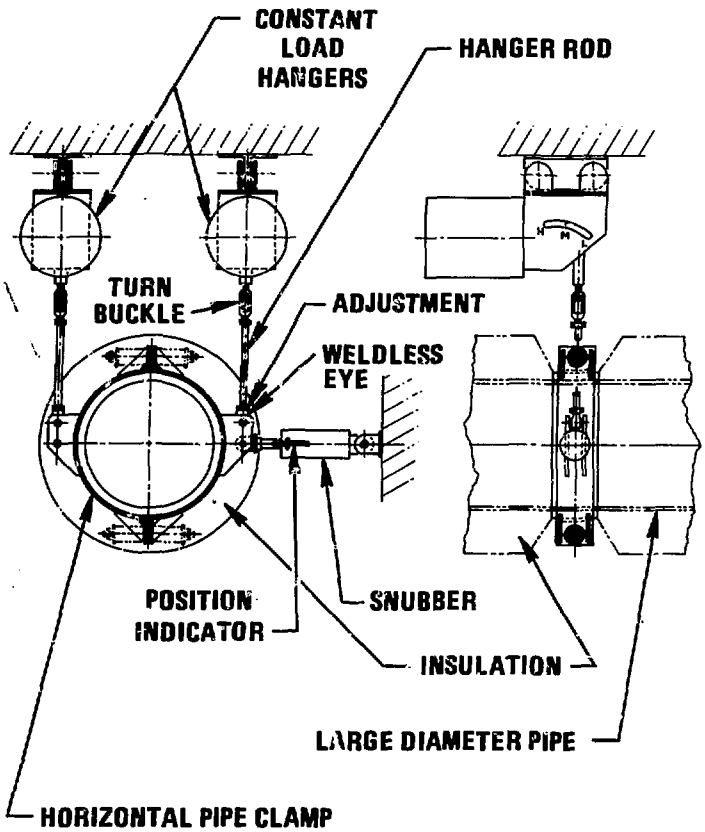

Figure 2 Typical Horizontal Piping Support Arrangement

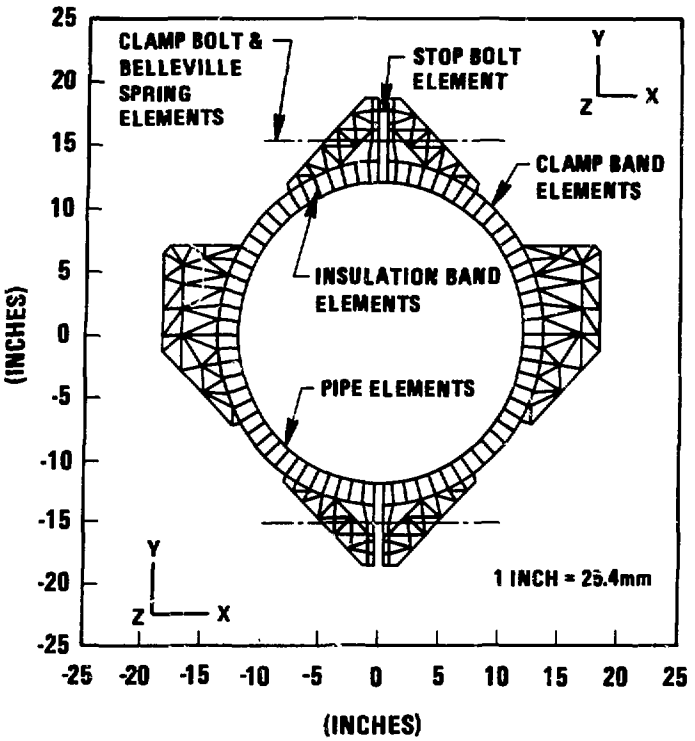

Figure 3 24-Inch (610 mm) Pipe/Clamp Interaction Model

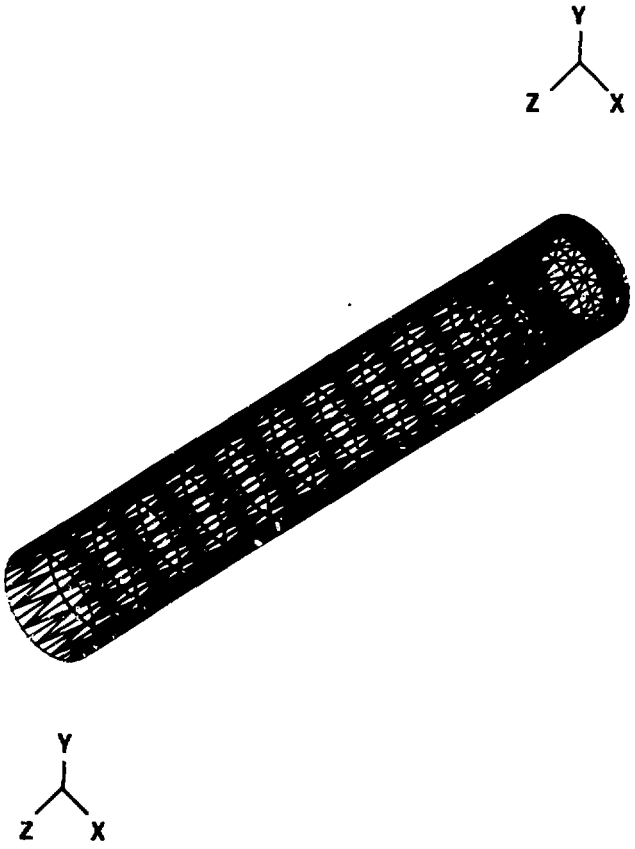

Figure 4 Full 3-D Shell Model of 24-Inch (610mm) Pipe

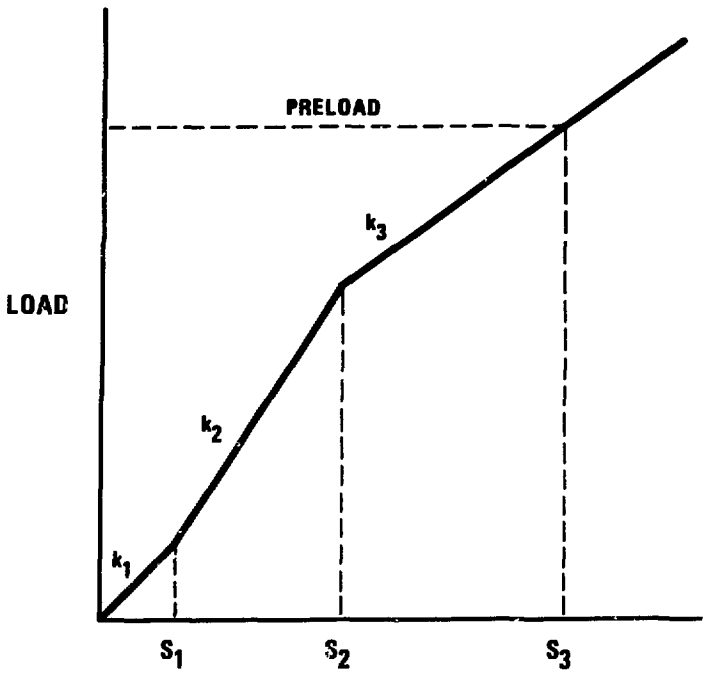

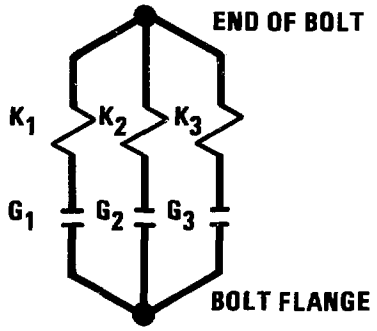

$K_1 = k_1$ $\quad G_1 = -S_3$

$K_2 = k_2 - k_1$ $\quad G_2 = S_1 - S_3$

$K_3 = k_3 - k_2$ $\quad G_3 = S_2 - S_3$

Figure 5 Belleville Spring Stackup Model

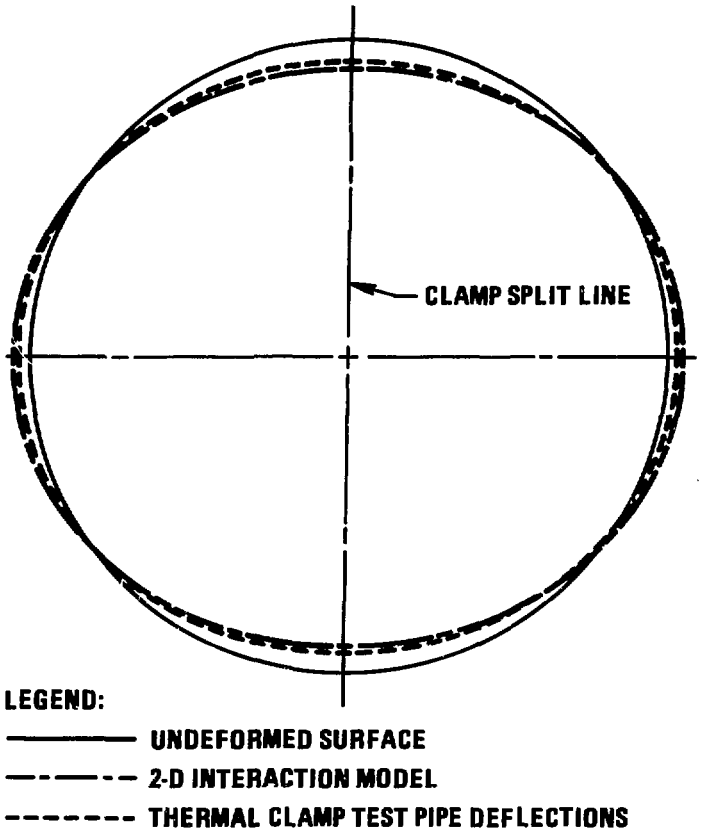

Figure 6 Comparison of 24" (610 mm) Pipe Wall Deflections for 2-D Clamp/Pipe Interaction Model to the Preliminary Thermal Clamp Test Data

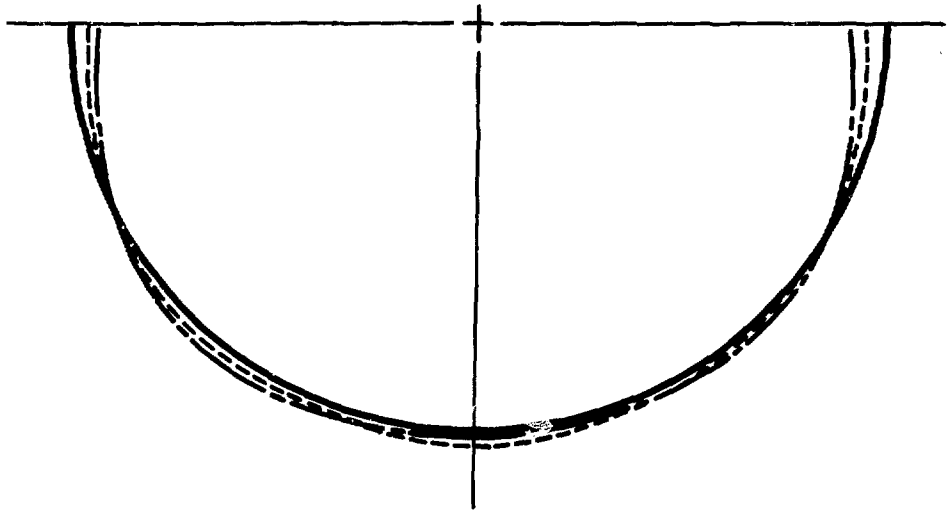

LEGEND:

UNDEFORMED SURFACE

SHELL MODEL DEFLECTIONS

2-D INTERACTION MODEL DEFLECTIONS

Figure 7 Comparison of Interaction Model Deflections and Shell Model Deflections for 24" x 6" (610mm x 12.7mm) Clamp Cold Preload Case

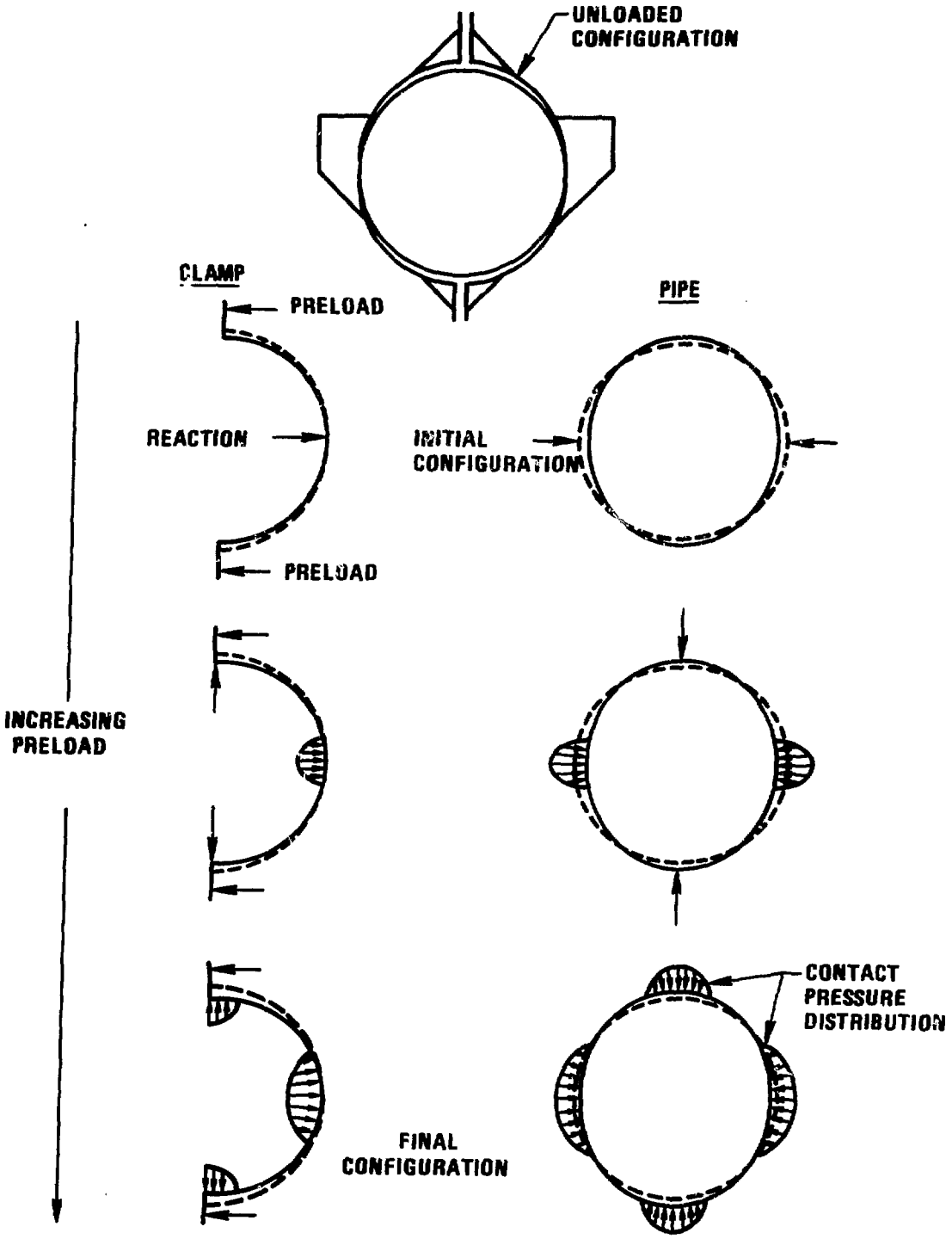

Figure 8 Deflections of Clamp and Pipe for Increasing Preloads

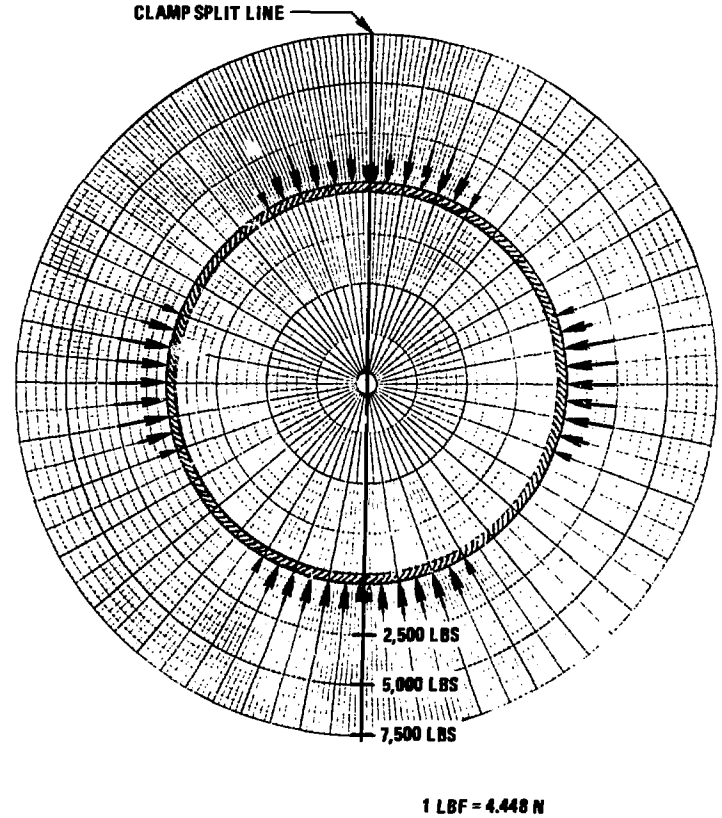

Figure 9 Interface Load Distribution for 24" x 6" (610mm x 150mm) Clamp-20,000 lbs (89,000 N) Cold Preload Case

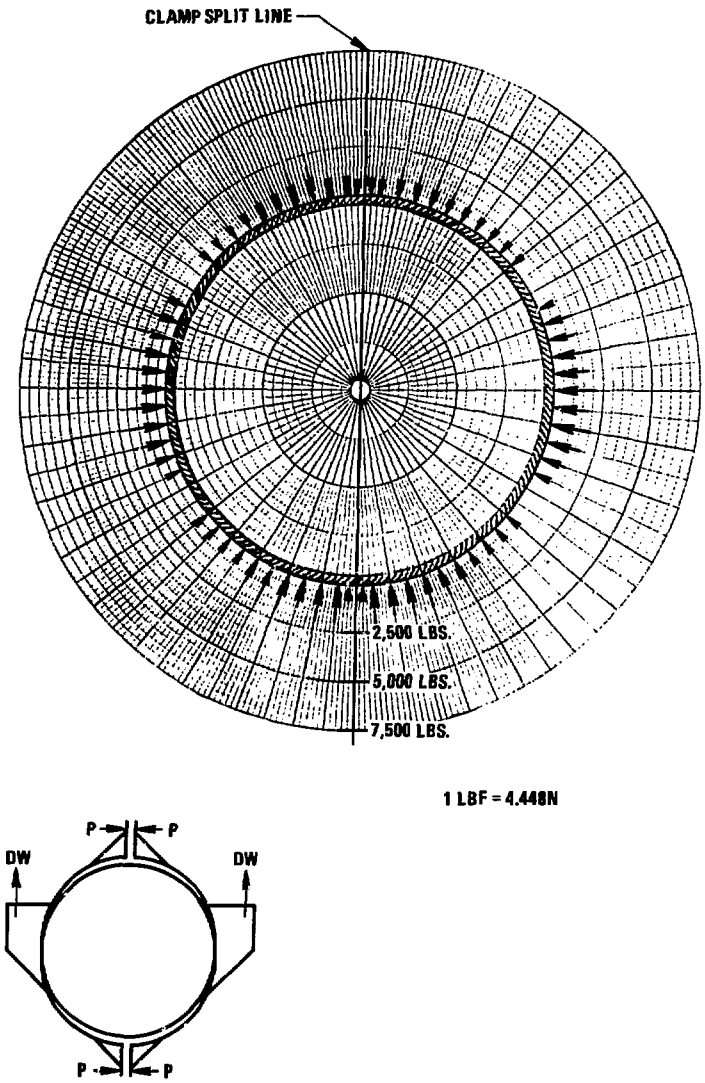

Figure 10. Interface Load Distribution for 24" x 6" (610mm x 150mm) Clamp – Preload + Thermal Expansion + 10,000 Lbs. (44,500N) Dead Weight Load

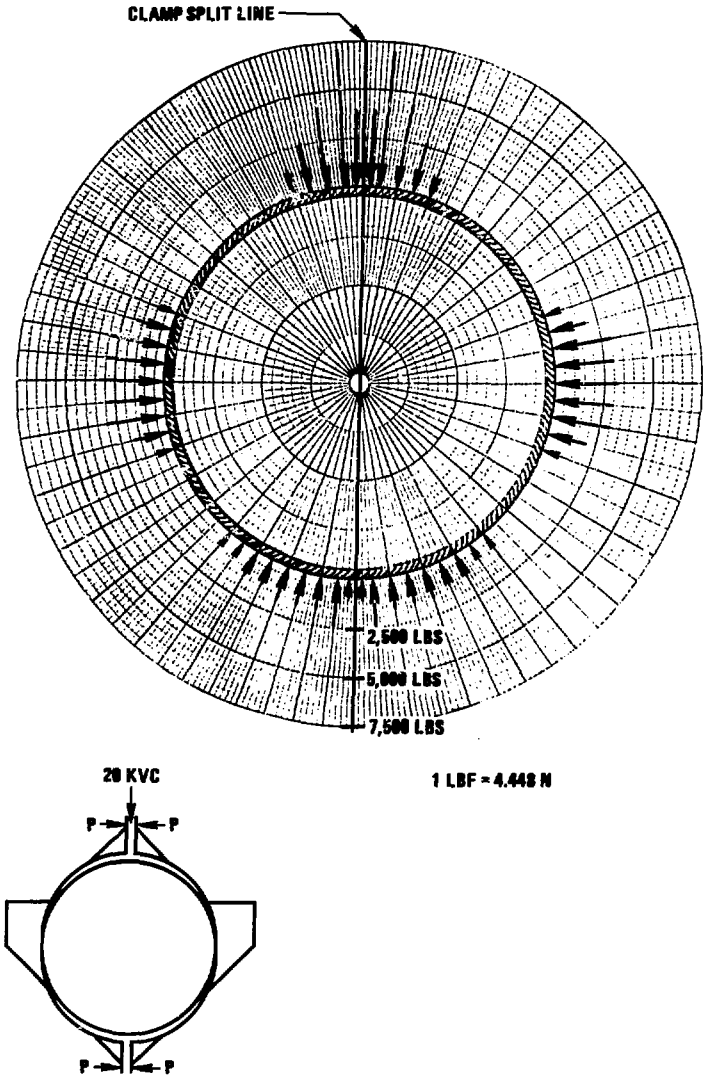

Figure 11 Interface Load Distribution for 24" x 6" (610mm x 150mm) Clamp Preload + Thermal Expansion + 20,000 Lbs (44,500N) Vertical, Compressive Load

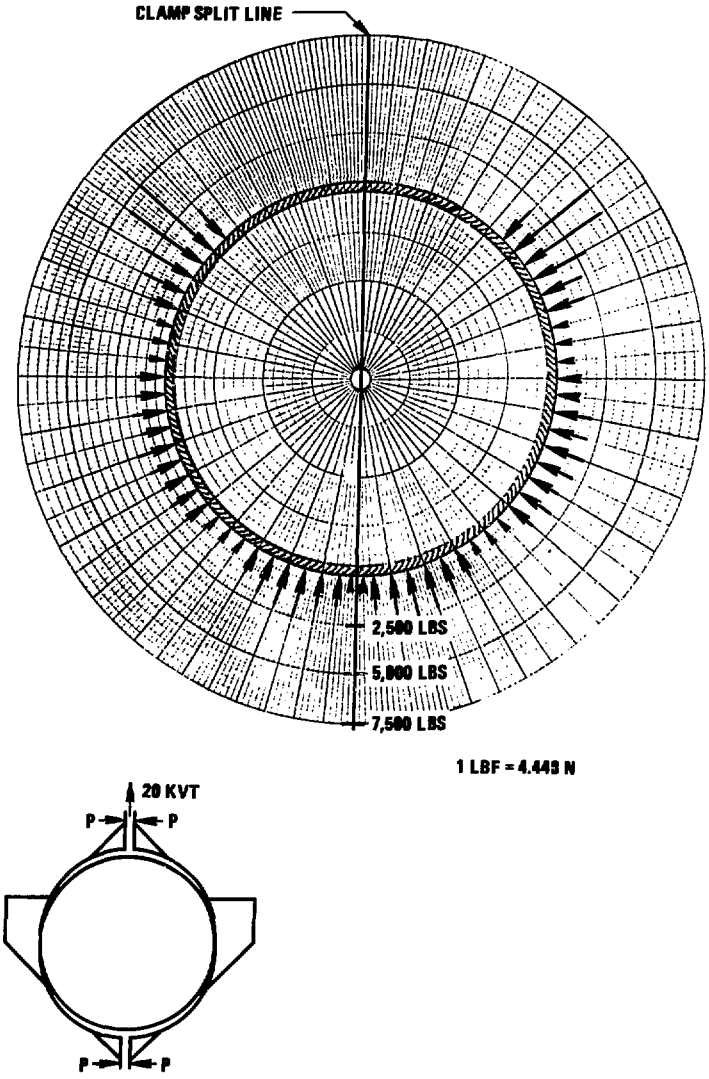

Figure 12 Interface Load Distribution for 24" x 6" (610mm x 150mm) Clamp Preload and Thermal Expansion + 20,000 Lbs (44,500 N)Vertical, Tensile Load

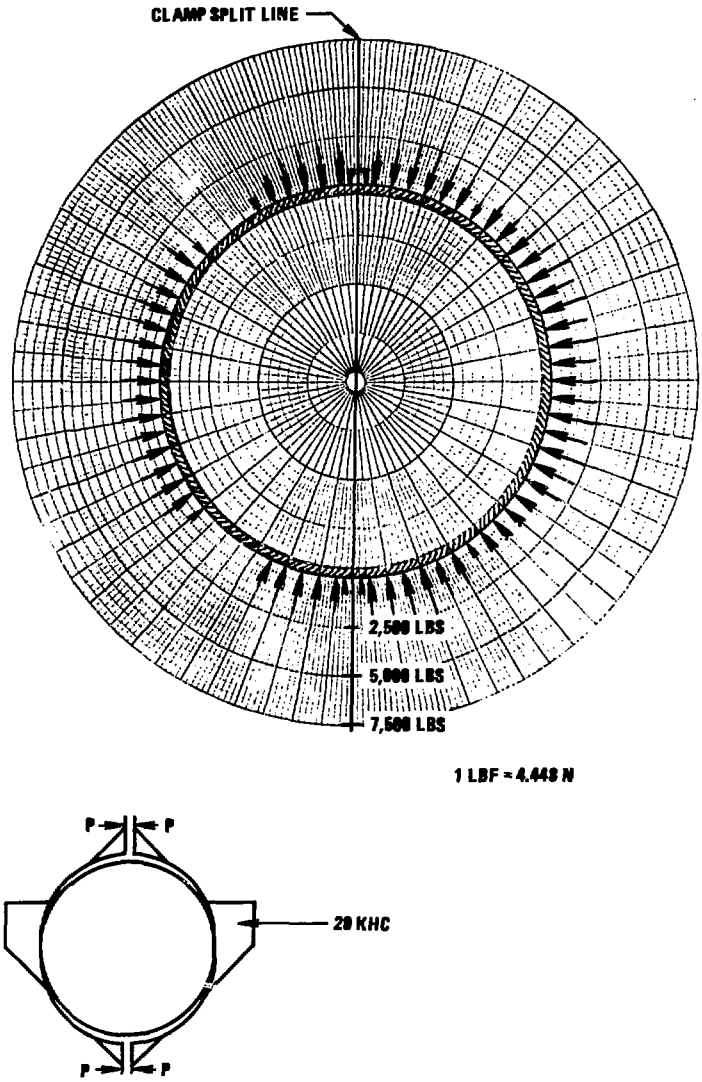

Figure 13 Interface Load Distribution for 24" x 6" (610mm x 150mm) Clamp
Preload and Thermal Expansion + 20,000 Lbs (44,500 N)
Horizontal, Compressive Load

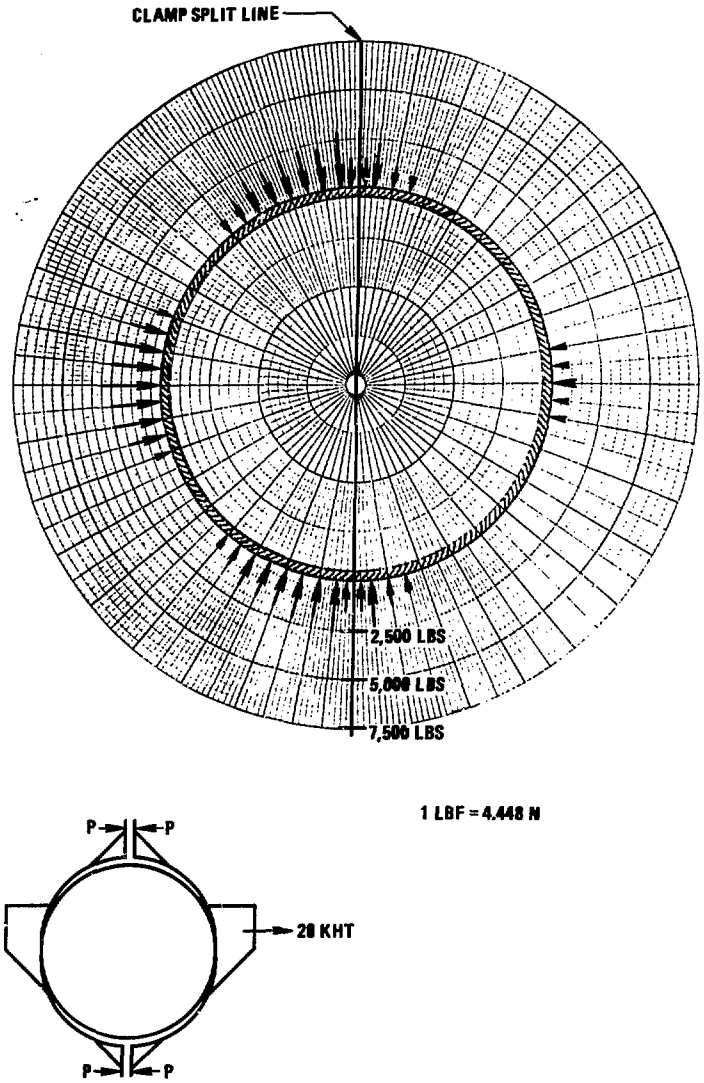

Figure 14 Interface Load Distribution for 24" x 6" (610mm x 150mm) Clamp Preload and Thermal Expansion + 20,000 Lbs (44,500 N) Horizontal, Tensile Load

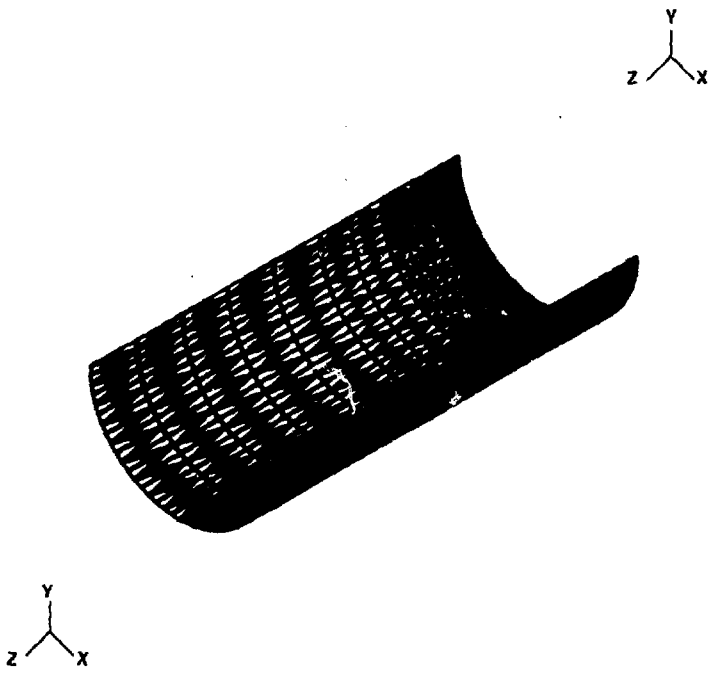

Figure 15 Refined 3-D Half Shell Model of 24-Inch (610mm) Pipe

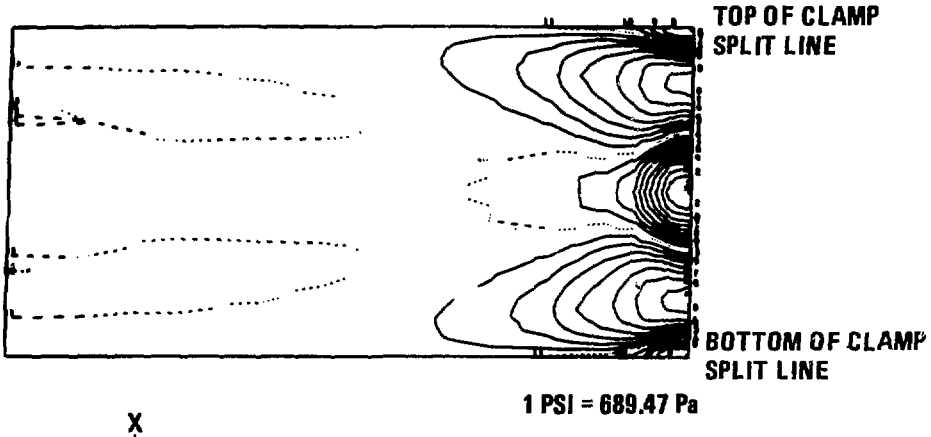

NO.	STRESS
MIN	−15087
1	−15000
2	−13500
3	−12000
4	−10500
5	−9000
6	−7500
7	−6000
8	−4500
9	−3000
10	−1500
11	0
12	1500
13	3000
14	4500
15	6000
16	7500
17	9000
18	10500
MAX	11345

Figure 16 Pipe Axial Stress Distribution at Outer Surface Due to Cold Boltup for 24" x 6" (610mm x 150mm) Clamp

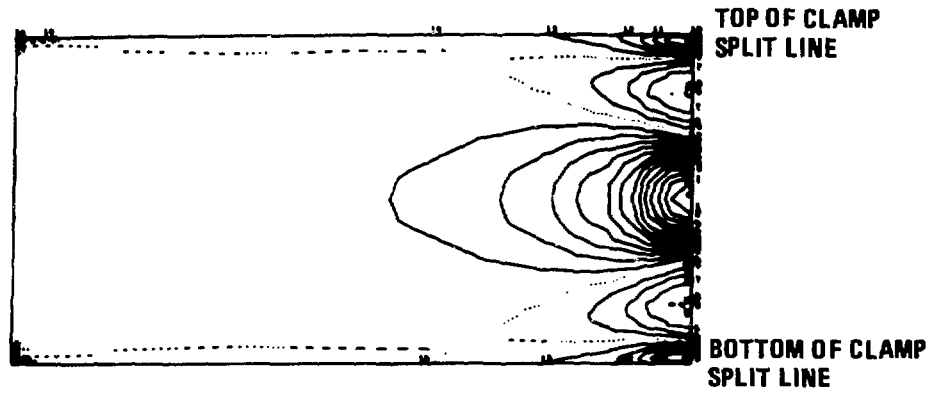

NO.	STRESS
MIN	−27839
1	−26000
2	−24000
3	−22000
4	−20000
5	−18000
6	−16000
7	−14000
8	−12000
9	−10000
10	−8000
11	−6000
12	−4000
13	−2000
14	0
15	2000
16	4000
17	6000
18	8000
MAX	8345

Figure 17 Pipe Hoop Stress Distribution at Outer Surface Due to Cold Boltup for 24" x 6" (610mm x 150mm) Clamp

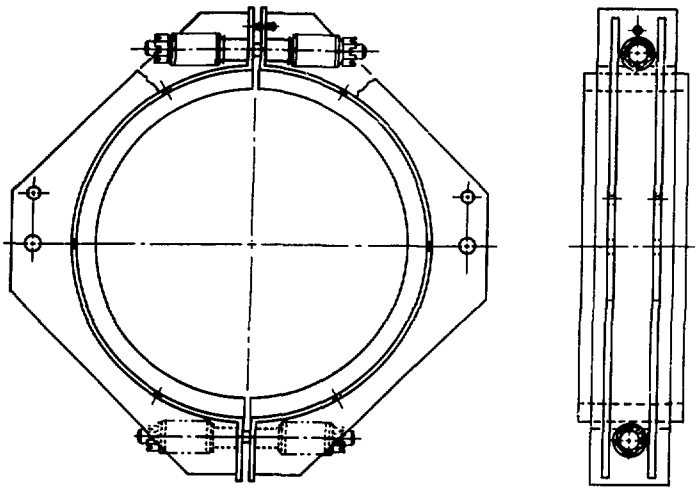

Figure 18 24-Inch (610mm) Revised Clamp Design